Detection and Quantized Conductance of Neutral Atoms Near a Charged Carbon Nanotube

Permanent link

Terms of Use

Share Your Story

Detection and Quantized Conductance of Neutral Atoms Near a Charged Carbon Nanotube

Trygve Ristroph, Anne Goodsell, J. A. Golovchenko, and Lene Vestergaard Hau

Department of Physics, Harvard University, Cambridge, Massachusetts 02138, USA
(Received 21 January 2004; published 17 February 2005)

We describe a novel single atom detector that uses the high electric field surrounding a charged single-walled carbon nanotube to attract and subsequently field-ionize neutral atoms. A theoretical study of the field-ionization tunneling rates for atomic trajectories in the attractive potential near a nanowire shows that a broadly applicable, high spatial resolution, low-power, neutral-atom detector with nearly 100% efficiency is realizable with present-day technology. Calculations also show that the system can provide the first opportunity to study quantized conductance phenomena when detecting cold neutral atoms with mean velocities less than 15 m/s.

The evolving ability to fabricate rigid micrometer and even nanometer scale structures allows for studies and utilization of atomic physics phenomena at length scales well below optical and cold-atom de Broglie wavelengths and for the miniaturization of atom traps and guides [1–7]. The success of many experiments and applications rests on the ability to confine and detect individual neutral atoms. Detection of neutral atoms has conventionally been achieved by optical fluorescence methods or via thermal ionization with a macroscopic hot wire followed by ion detection and counting. The spatial resolution of optical methods is set by the diffraction limit of light, and small optical cross sections often preclude the study of single atoms. Hot-wire ionization detection is capable of revealing small numbers of atoms with small ionization potentials, but the spatial resolution is limited by the size of the wire and surface diffusion during the residence time on the wire before ionization occurs. Also, the high temperature of thermally ionized atoms suppresses the energy resolution of the system. Recently, low-voltage field-ionization detection based on continuous current measurements on gaseous samples using the tips of densely packed multi-walled carbon nanotubes has been demonstrated [8,9].

In this Letter, we propose an atom detector based on a single-walled carbon nanotube (SWNT) that surpasses conventional detection methods in terms of simplicity, sensitivity, resolution, and size, and whose fundamental properties are worthy of theoretical and experimental investigation. The nanotube-based system builds on earlier studies of atom-wire interactions that considered atom quantum dynamics in a $1/r^2$ potential created by a small wire [1]. Experiments have been performed using large-diameter metallic wires and the thermal ionization that reveal expected results in the classical regime [10], but as yet neither a broadly applicable neutral-atom detector nor the fundamental quantum mechanical issues and potentialities raised in initial theoretical studies have been realized. We describe below a voltage-biased SWNT atom detector that provides the two essential new ingredients important to both possibilities: high electrical fields capable of cap-

turing neutral polarizable atoms and subsequently inducing field-ionization enabling single atom detection, and wire diameters much smaller than cold-atom de Broglie wavelengths which will enable the detector to reveal quantized conductance of neutral atoms for the first time.

The proposed detector and experimental setup is depicted in Fig. 1. Rubidium atoms derived from a thermal vapor source are laser cooled and directed towards a charged single-walled carbon nanotube. Cren *et al.* developed an intense (10^{11} atoms/cm^2/s) sub-milli-Kelvin cold-atom beam with launching velocities (~0.3–3 m/s) that can be controlled by the relative frequency detuning between two pairs of laser beams [11]. We assume such a beam in our calculations. The cold-atom beam is directed onto a freestanding SWNT, which is electrically contacted at both ends and coaxially shielded with a grounded cylindrical grid. Such a nanotube device can now be readily fashioned with photolithography, metal evaporation, and chemical vapor deposition techniques [12]. A typical tube with a 1 nm radius biased to roughly 50 V achieves the 3 V/nm field required for efficient rubidium field ionization [13]. Detection of the resultant ions emanating from the SWNT is effected with nearly
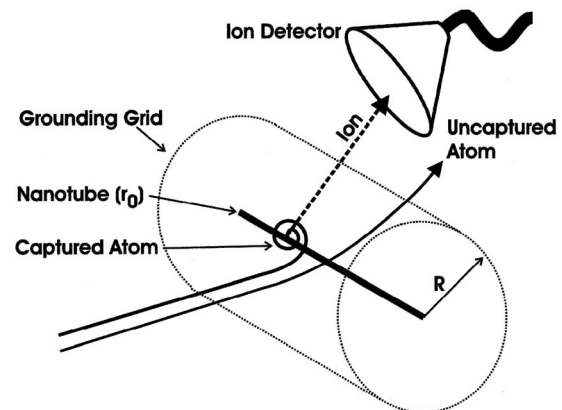

FIG. 1. Schematic of experimental setup.

066102-1

100% efficiency with a nearby electron multiplier device such as a channeltron or multichannel plate. Under these conditions counting rates of order 10^4 ions/s can be realized using the cold-atom beam described above and a nanotube only 5 μm long. This is more than adequate to reveal the physics described below.

Discrete quantum steps should exist in the cross section for atom capture (or matter wave conductance) versus voltage, for a very thin wire [14,15]. The phenomenon is aptly called the "angular momentum quantum ladder" since the sharp steps result from angular momentum quantization in the $1/r^2$ polarization potential attracting the atoms to the wire. (See Fig. 2.) Observation of these steps would be the first demonstration of quantized conductance for a neutral polarizable particle system. An alternative technique to measure the quantized conductance of neutral particles has been proposed [16], but at this time the effect has been observed only for two-dimensional Fermi electron gases in solid-state quantum devices [17]. A related effect has been observed in phonon transport at low temperatures [18].

In the family of attractive $1/r^n$ potentials, $n = 2$ lies at the boundary between potentials with finite ground-state energies and those that are unbounded from below [19]. The potential energy of a neutral polarizable atom in a static electric field, E, is given by $-\alpha E(r)^2/2$, where α is the static atomic polarizability and r the atom position. This leads to an inverse square law dependence for an infinitely long charged wire. Using a wire of radius r_0 charged to voltage V_0 with respect to an outer grounding cylinder of radius R, one finds the effective potential energy for the classical radial motion to be

$$U_r(r) = \frac{L^2}{2mr^2} - \frac{K^2}{2mr^2}.$$

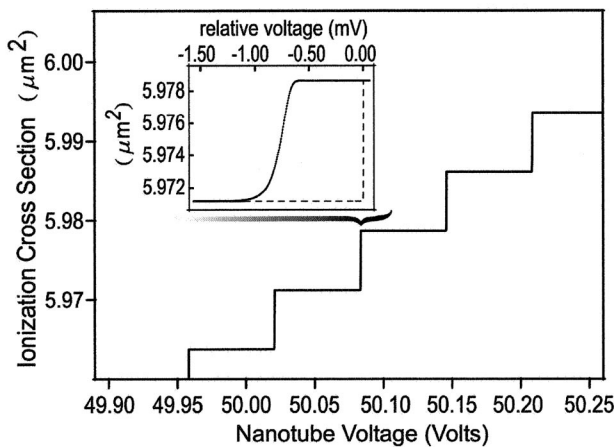The first term is the repulsive centrifugal barrier, with L the

FIG. 2.   Calculated steps in the angular momentum quantum ladder. The nanotube diameter is 2 nm and the length is 5 μm. Inset shows contribution from quantum tunneling of uncaptured atoms for a 1 m/s atomic beam.

conserved angular momentum of the atomic motion in a plane perpendicular to the nanotube, and m the atomic mass. The second term is the potential energy due to the induced polarization, and $K^2 = \alpha V_0^2 m / \ln^2(R/r_0)$. Evidently, the effective potential energy for radial motion has exactly the inverse square law discussed above.

We call K the critical angular momentum. For $L > K$ the atom experiences a repulsive radial potential dominated by the centrifugal potential. Atoms with $L < K$ experience an attractive radial potential dominated by the polarization interaction and will be captured by the nanotube. For an atom with velocity ν, the corresponding classical critical impact parameter for capture is given by $b_c(\nu) = K/m\nu$, which is typically on the micron scale for cold atoms. Captured atoms spiral in and will collide with the nanotube if they are not ionized first.

Increasing the nanotube voltage results in the capture of atoms with increasingly large angular momenta. Assuming all captured atoms ionize, the classical ionization cross section is linear in V_0 and is given by $\sigma = 2b_c(\nu)l_{nt}$, where l_{nt} is the length of the nanotube. We note that in all cases of interest here captured states are not bound states, rather they have positive kinetic energy far from the nanowire. The angular momentum of these states is quantized and the cross section for capture and ionization is therefore expected to increase in discrete steps as each new angular momentum state is captured with increasing voltage. A full quantum mechanical treatment bears out this argument [14,15]. When the wire diameter is comparable to the (initial) reduced de Broglie wavelength of the atom, $\lambdabar_B$, the steps will be sharp and easily resolvable. For cold atoms, the step spacing is independent of incident atomic velocities and is equal to $\Delta V_{step} = \hbar \ln(R/r_0)/\sqrt{\alpha m}$, which is 62.5 mV for rubidium atoms and the geometry described above. The weak logarithmic dependence on the ratio of geometric factors, $R/r_0 = 10^7$, suggests a new way to measure α. The step height is $\Delta\sigma_{step} = 2\lambdabar_B l_{nt}$, as shown in Fig. 2, which we have computed for rubidium atoms incident on the nanotube with an initial velocity of 1 m/s and a 5 μm long nanotube.

The steps are not expected to be infinitely sharp because the atomic wave function components with $L > K$ can tunnel into the ionizing region despite the fact that they are not actually captured. To estimate the ionization contribution of uncaptured atoms, we radially integrated the voltage dependent product of suitably normalized radial atom probability densities (from Schrödinger-equation eigenfunctions) for $L = K + \hbar$ and $L = K + 2\hbar$ with the ionization rate. Only $L = K + \hbar$ has any significant contribution. Tunneling leads to a shift of the step edge position by about 0.6 mV, or 1% of the step width, and broadens the rising edge about 0.25 mV, or 0.4% of the step width. The effects are so small as to be only evident in the expanded inset of Fig. 2, where the relative voltage is reckoned with respect to the capture voltage at $L = K$.

With increasing atomic velocities, these effects become larger but the step modulations are still discernible for velocities less than 15 m/s; above this threshold, the smearing becomes comparable to the step size and the result is that the high-velocity capture cross section approaches the classically expected one, despite the fact that it cannot be explained as the result of $\hbar \to 0$.

The emitted current of ionized atoms is directly proportional to the cross section expressed in Fig. 2 and can be compared to the quantized current observed as a function of gate voltage across a 2D quantum point contact (QPC). In both cases the effective width of the conducting channel is modulated with a voltage, and the wave nature of the particles gives rise to steps in the current. However, there are several interesting and important differences: (i) the steps arise from quantization of transverse momentum in the conducting channel for a QPC, and from quantization of *angular* momentum when atoms are "funneled" into a charged nanotube; (ii) the step *height* for a QPC system is simply determined by fundamental constants and bias voltage because the density of states for a 2D Fermi gas is constant, whereas the step height for the nanotube system is dependent on atomic beam density but not beam velocity or voltage; (iii) the voltage step *width* depends on the geometry of the gate electrode for a QPC, but for a nanotube the step width depends only on the fundamental constants of the system, independent of beam parameters.

To calculate the field-ionization rate as a function of electric field we use a WKB based approach for the tunneling rate for an atomic electron into an unbound state

Ionization Probability

FIG. 3. Ionization probability versus angular momentum and voltage for 1 m/s rubidium atoms incident on a 2 nm diameter nanotube.

during the atoms's approach to the wire [13]. Figure 3 shows the calculated ionization probability versus V_0 and L for rubidium atoms impinging on a 2 nm diameter nanotube. The white region indicates complete capture and ionization, and the black none at all. The linearity of the capture cross section with voltage is clear from the straight (sloping) boundary between white and black on the right. We call this the capture boundary. The anticipated quantum steps shown in Fig. 2 are a fine structure effect along the capture boundary and are not visible in Fig. 3. Atoms with $L > K$ contribute to the black region on the right; these atoms are not captured and are unlikely to ionize. If the voltage is high enough (greater than ~ 45 V), captured atoms will field ionize regardless of their angular momentum. At lower voltages, only high angular momentum captured atoms move radially through the field slowly enough to be ionized before hitting the surface of the tube. This explains both the dense black region on the left and the sharp white feature along the low-voltage capture boundary.

An experimental study of the energy distribution of the ejected ions will also allow the possibility of angular momentum selection or identification for a captured atom and yield experimental insight into the details of the nanoscale tunneling process and the nanotube–neutral-atom interactions. The major contribution to the final kinetic energy of the outgoing ion is determined by the electrostatic potential at the position where ionization actually takes place. An atom with low angular momentum can approach a higher electrostatic potential region before it is ionized, and hence the ion kinetic energy per charge should be closer to the applied voltage on the nanotube than for high angular momentum trajectories. Our calculations show that ions derived from atoms with L between ~ 0.8 and $1.0K$ have an average energy about 0.5 eV less than those with L less than $\sim 0.8K$.

Not included in our calculations is the fact that the energy distribution of ejected ions will be influenced by interference effects associated with quantum reflection of tunneling electrons at the surface of the nanotube. The electron transmission coefficient through the tunneling barrier between the atom and the nanotube is most likely an oscillatory function of the radial distance between the atom and the nanotube. Thus we expect oscillations in the ion energy distribution similar to those observed in a tunneling microscope [20] or field ion microscope [21]. Bound-image electronic states, which have been recently predicted [22], will also play a role in the tunneling rate, and this system may offer a unique way to detect such states. Note that the energy distribution may depend on the time dependent local electron transport properties of the nanotube itself. For every ion created, there is an electron injected into an available electronic state in the nanotube, and the dynamics of that charge in the tube may influence the ion's final energy. At low voltages where ionization
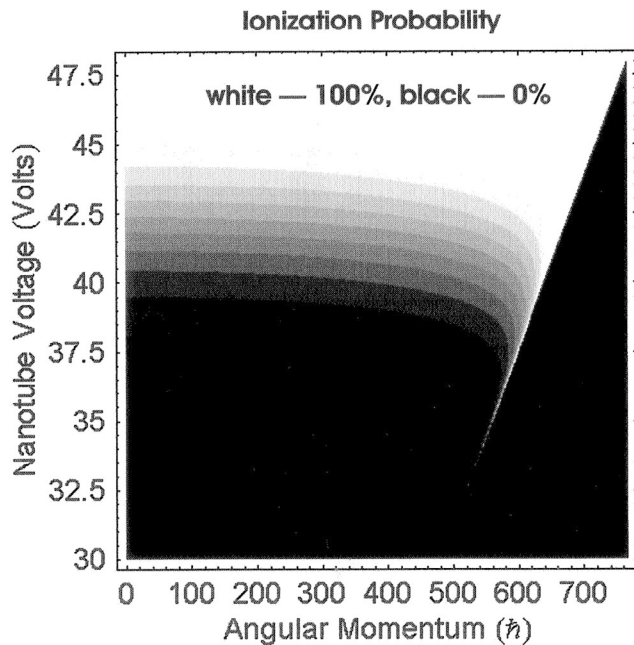
occurs near the nanotube surface, the ion energy distribution will be sensitive to the nanotube structure (including charged defects) and in fact may be a unique way to probe it.

The prospect of extending atom-nanotube studies to optically pumped atoms is very attractive. The differences between the polarizabilities and ionization energies of ground- and excited-state rubidium atoms leads to significantly enhanced capture dynamics and electron tunneling probabilities. In addition to enhancing capture cross sections and ionization probabilities, this can provide a detection method for the recently predicted ''Purcell effect'' near carbon nanotubes [23]. The Stark shift of an atom has a rapid spatial variation near a charged nanotube and can be used to spatially probe the optical activity of captured atoms through coincidence measurements of optical fluorescent scattering and ionization events as a function of laser wavelength.

Furthermore, the time correlation of individual ionization events, which is accessible at high bandwidths using an electron multiplier ion detector, will be worthy of study with the new detector and high-density degenerate, cold atomic gases. These correlations will be determined by atom-atom interactions and statistics [24], e.g, van der Waals forces, quantum Casimir forces, and the statistics of identical particles (bosons or fermions). Notwithstanding the richness of the novel quantum effects accessible with cold atoms discussed here, the device may well prove most useful as an efficient, high spatial resolution single atom detector, particularly when using long nanotubes and higher velocity atoms.

[1] Lene Vestergaard Hau, M. M. Burns, and J. A. Golovchenko, Phys. Rev. A **45**, 6468 (1992).

[2] Lene Vestergaard Hau, J. A. Golovchenko, and Michael M. Burns, Phys. Rev. Lett. **74**, 3138 (1995).

[3] J. D. Weinstein and K. G. Libbrecht, Phys. Rev. A **52**, 4004 (1995).

[4] J. Schmiedmayer, Appl. Phys. B **60**, 169 (1995).

[5] M. Drndíc, K. S. Johnson, J. H. Thywissen, M. Prentiss, and R. M. Westervelt, Appl. Phys. Lett. **72**, 2906 (1998).

[6] J. Reichel, W. Hänsel, and T. W. Hänsch, Phys. Rev. Lett. **83**, 3398 (1999).

[7] Dirk Müller, Dana Z. Anderson, Randal J. Grow, Peter D. D. Schwindy, and Eric A. Cornell, Phys. Rev. Lett. **83**, 5194 (1999).

[8] David J. Riley, Mark Mann, Donald A. MacLaren, Paul C. Dastoor, William Allison, Kenneth B. K. Teo, Gahan A. J. Amaratunga, and William Milne, Nano Lett. **3**, 1455 (2003).

[9] Ashigh Modi, Nikhil Koratkar, Bingqing Wei, and Pulickel M. Ajayan, Nature (London) **424**, 171 (2003).

[10] Johannes Denschlag, Gerhard Umhaus, and Jörg Schmiedmayer, Phys. Rev. Lett. **81**, 737 (1998).

[11] P. Cren, C. F. Roos, A. Aclan, J. Dalibard, and D. Guéry-Odelin, Eur. Phys. J. D **20**, 107 (2002).

[12] H. B. Peng, T. G. Ristroph, G. M. Schurmann, G. M. King, Joonah Yoon, V. Narayanamurti, and J. A. Golovchenko, Appl. Phys. Lett. **83**, 4238 (2003).

[13] Dimitri Fisher, Yitzhak Maron, and Lev P. Pitaevskii, Phys. Rev. A **58**, 2214 (1998).

[14] Lene Vestergaard Hau, B. D. Busch, Chien Liu, Michael M. Burns, and J. A. Golovchenko, in *Proceedings of the Twentieth International Conference on the Physics of Electronic and Atomic Collisions, Vienna, Austria, 1997*, edited by F. Aumayr and H. P. Winter (World Scientific, Singapore, 1998).

[15] J. Denschlag and J. Schmiedmayer, Europhys. Lett. **38**, 405 (1997).

[16] J. H. Thywissen, R. M. Westervelt, and M. Prentiss, Phys. Rev. Lett. **83**, 3762 (1999).

[17] B. J. van Wees, H. van Houten, C. W. Beenakker, J. G. Williamson, L. P. Kouwenhoven, D. van der Marel, and C. T. Foxon, Phys. Rev. Lett. **60**, 848 (1988).

[18] K. Schwab, E. A. Henriksen, J. M. Worlock, and M. L. Roukes, Nature (London) **404**, 974 (2000).

[19] L. D. Landau and E. M. Lifshitz, *Quantum Mechanics* (Pergamon, Oxford, 1977), pp. 54, 114–117.

[20] R. S. Becker, J. A. Golovchenko, and B. S. Swartzentruber, Phys. Rev. Lett. **55**, 987 (1985).

[21] Andrew J. Jason, Phys. Rev. **156**, 266 (1967).

[22] Brian E. Granger, Petr Král, H. R. Sadeghpour, and Moshe Shapiro, Phys. Rev. Lett. **89**, 135506 (2002).

[23] I. V. Bondarev, G. Ya. Slepyan, and S. A. Maksimenko, Phys. Rev. Lett. **89**, 115504 (2002).

[24] Masami Yasuda and Fujio Shimizu, Phys. Rev. Lett. **77**, 3090 (1996).